Molecular Crystals and Liquid Crystals
Publication details, including instructions for authors and subscription information:
http://www.tandfonline.com/loi/gmcl20

Photoinduced Molecular Reorientation and Relaxation in a Liquid Crystalline Polymer

S. Arisi [a], P. Camorani [a], L. Cristofolini [a], M. P. Fontana [a] & M. Laus [b]

[a] Dipartimento di Fisica and INFM, Università di Parma, Italy

[b] Dipartimento di Chimica Industriale, Università di Bologna, Bologna, Italy

Version of record first published: 29 Oct 2010

To cite this article: S. Arisi, P. Camorani, L. Cristofolini, M. P. Fontana & M. Laus (2002): Photoinduced Molecular Reorientation and Relaxation in a Liquid Crystalline Polymer, Molecular Crystals and Liquid Crystals, 372:1, 241-253

To link to this article: http://dx.doi.org/10.1080/10587250127575

Mol. Cryst. and Liq. Cryst., 2001, Vol. 372, pp. 241-253

Photoinduced Molecular Reorientation and Relaxation in a Liquid Crystalline Polymer

S. ARISI[1], P. CAMORANI[1], L. CRISTOFOLINI[1], M. P. FONTANA[1] and M. LAUS[2]

[1]*Dipartimento di Fisica and INFM, Universitá di Parma, Italy and*
[2]*Dipartimento di Chimica Industriale, Universitá di Bologna, Bologna, Italy*

Abstract

In this paper we present a study of photoinduced effects, including molecular relaxation in a side chain liquid crystalline polymer. In particular, we have studied relaxation phenomena using Ellipsometry and Photoinduced Birefringence in pump-probe experiments, which were carried out as a function of temperature, optical pump intensity and sample preparation and history. Two specific areas were investigated in detail: the frustration effect of the trans-cis photoisomerization transition on the nematic phase, and hence the photoinduced isothermal transition from perturbed nematic to a totally frustrated (isotropic) phase; and the approach of the glass transition, in such a fragile polymeric glass as the one we studied.

keywords:polymeric liquid crystals, birefringence, ellipsometry, glass-transition.

1 Introduction

In the last decade, much effort has been devoted to the study of photosensitive side chain polymers. Such materials are deemed to have quite interesting applications to optoelectronics, non-linear optics, high density optical memories etc.[1]. Within this group particularly interesting are liquid crystalline side chain polymers[2], which conjugate the useful characteristics of low molecular weight liquid crystals with the easy workability and stability of polymer plastics. Given such premises, much emphasis was given to the study of optically-induced molecular reorientation through the trans-cis isomerization transition [3], and to the potential of such effects for applications to optical writing and information storage down to the molecular level [4]. The materials also feature a rich and complex phenomenology, which makes them very interesting also from a fundamental point of view. Their dynamics is the result of the interplay between several types of interactions and processes: the mesogenic potential, the conformational main chain transitions, the glass transition, the molecular trans-cis isomerization. The relative weight of such processes depends of course on temperature, but apart from that it can be externally influenced by optical pumping with light of the appropriate wavelength, polarization and intensity. Furthermore, as we shall propose, the system may be viewed as being composed of two fluids, with dynamical relaxation taking place over very different time scales: the mesogenic side chains and the polymeric main chain. It is expected that some coupling between such fluids should however exist, and this would strongly influence the time development of the photoinduced effects; furthermore, such coupled two fluid system could model the α and β relaxations of glass transition phenomenology[5] and theory[6].

In this paper we present a study of photo-induced molecular reorientation and relaxation in the equilibrium and optically induced phases in photosensitive liquid

crystalline polymers. By appropriate variation of optical pumping characteristics, we can modulate the relative weight of the aforementioned interactions and processes, and thus alter the phase transition behavior in a controlled fashion. Particularly interesting are the frustration effects of trans-cis cycling on the nematic phase[7], memory effects after optical pumping, and the photo-induced slow relaxations in the neighborhood of the glass transition, which we have probed by photoinduced birefringence measurements in the transmission mode, and by null-ellipsometry in reflection mode. The experiments were performed as a function of temperature, time, pump light intensity and wavelength, and thermal and optical cycling of the sample.

In previous papers we have shown the feasibility of using Fluctuation Raman Spectroscopy (FRS) to monitor the optically induced molecular reorientational effects and the sensitivity of the viscoelastic properties of the sample to optical pumping[8, 9]. Such measurements were performed mainly on cast solution thick samples ($\approx 1\mu m$); thus the use of FRS in the micro mode was essential to insure optical homogeneity. With the present work we extend the range of samples we have studied: the measurements in fact were performed not only on cast solution films, but also on molecular mono- and multilayers deposited with the Langmuir-Schaeffer technique [10]. Thus we were able to check the effects of different sample morphology and order on the relaxation behavior. A preliminary report on the behaviour of LS multilayers of PA4 in the vicinity of the glass transition can be found in [11].

Finally, our thermal cycling experiments have revealed extensive memory effects in the optically treated samples, which may be used to orient the side chain molecules even after the sample has been heated up to the true isotropic phase. Such effects appear to be due to an interplay between the orientational dynamics of the side chains and the conformational motions of the main chain, hence yielding support to the coupled two fluid modeling of our system.

2 Materials

In the present study we employed a prototype azo-polymer: Poly[[4-pentyloxy-3'-methyl-4'(6-acryloxyexyloxy)]azobenzene] (henceforth labeled PA4); however the phenomenology reported here was observed in other members of this LCP family. The azobenzene mesogenic moiety is attached to the acrylate main chain via a 6 member methylene flexible spacer. The synthesis and general properties of this class of polymer are described elsewhere[12]. Here we recall that the material we used has a 4 member alkyl tail and this yields a nematic phase with a melting point of 83°C and a clearing point of 96°C upon heating. Upon cooling the nematic phase strongly undercools all the way to room temperature to a glassy phase ($T_g \approx 21°C$)[12]. We also recall that there are aging effects which indicate possible nucleation of smectic-like or microcrystalline phases in the neighborhood of 60°C[13]. As already stated, the samples were prepared by the cast solution technique, yielding reasonably homogeneous films of thicknesses in the 1-3μm range, and by the Langmuir-Schaeffer technique, which yielded high quality, homogeneous molecular mono- and multilayers.

3 Induced Birefringence

Liquid crystals are optically anisotropic, and this gives rise to a variety of optical effects in polarized light [14]. Such effects can be externally controlled, by either rotating the nematic axis, or by varying the index of refraction anisotropy. In the specific case we are considering, both methods can be used.

The trans-cis isomerization process under polarized light excitation can be quite an efficient optical pump to modify the molecular orientational distribution [15]. In fact, the side chain azobenzene molecules whose main symmetry axis has a non-zero component along the polarization vector $\vec{E}$ of the incident light will reorient after undergoing a trans-cis-trans isomerization cycle: those molecules which end up oriented in the plane perpendicular to $\vec{E}$ will not absorb light any longer and hence remain there, whereas the others will cycle again and again, until a stationary state is reached, in which a considerable fraction of the side chain moieties will be oriented perpendicularly to $\vec{E}$ [16].

In PA4, for sufficiently high incident power density ($\approx$100mW/cm^2) essentially all the azobenzene side chains are reoriented, forming a sort of monodomain, optically anisotropic system with the main optic axis parallel to $\vec{E}$ (and negative birefringence). The process will depend on the amount of energy absorbed, i.e. on the intensity, wavelength and duration of the optical pump. It will also depend on temperature: because of the cis-trans back relaxation process, and because of the temperature dependence of the equilibrium nematic ordering. The relaxation after optical pumping is turned off will also depend on the conformational dynamics in the main chain, and on the vicinity of the glass transition. Finally, a further complication is due to the "poisoning" effect of the optical pumping [7], which by increasing the population of non-mesogenic cis molecules, can actually frustrate the occurrence of the nematic phase, leading to an optically induced isotropic phase at a temperature T_p which will depend on the pump light power. Let us recall however that this isotropic "phase" concerns only the nematic fluid, which will coexist with the polymeric main chain fluid, in which the main chain conformation may have been influenced by the forced reorientation of the side chains.

This very complex phenomenology can be studied by monitoring light-induced changes in the sample optical anisotropy in a pump probe configuration. We have done this both in the standard transmission mode, and in the reflection ellipsometric mode. The ellipsometric data were taken both with single wavelength excitation and spectroscopically. In this paper we shall discuss mainly the spectroscopic measurements; the detailed single wavelength data are presented elsewhere [11]. With the exception of the spectroscopic ellipsometry, the probe is a polarized He-Ne laser beam (power $\approx$ 2mW, wavelength λ=633nm) which in principle is not absorbed by the material. Optical pumping is provided by a polarized Ar^+ beam (power density $1 \sim 200$mW/cm^2). The pumping wavelength was varied between 514.5nm and 458nm,thus spanning the tail of the azobenzene characteristic absorption region [3]. In figure 1 we report the anisotropy of the optical absorbance due to the trans isomer of a sample that was previously alligned by means of optical pumping with light polarized in the 0° direction. Our result clearly indicates that the azobenzene moieties lye oriented perpendicularly to the direction of

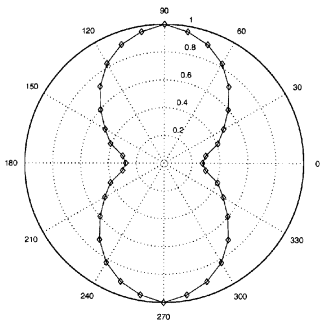

Figure 1: Anisotropy of the optical absorbance due to the trans isomer. The sample was previously alligned by means of optical pumping with light polarized in the 0° direction.

polarization of the pump light.

For the Photoinduced Birefringency experiments in transmission mode, the probe beam after passing through the sample and a 0.5mm pinhole is split by a Wollaston prism into the two polarized components $I_\perp$ and $I_\parallel$ and subsequently detected with two photodiodes. The signal is then fed into a computer. The pump beam is almost collinear with the probe beam and is polarized at 45° to its polarization. In this geometry the induced birefringence signal is maximized. If now the optic axis changes its orientation or the index of refraction anisotropy changes due to the molecular relaxation processes (either photoinduced or back to equilibrium), the ratio of the two components will vary in time and from such variation the connected phase retardation change can by obtained [17]: $\Delta\varphi = 2\pi\lambda\Delta n/d = arctan(\sqrt{(I_\perp/I_\parallel)})$ where d is the sample thickness, λ the probe wavelength (633nm) and Δn is the index of refraction anisotropy. This is the basic quantity we shall use in discussing the photoinduced relaxation phenomena in the transmission mode.

3.1 Results from induced birefringence

The first photoinduced effect we wish to consider is the poisoning of the nematic phase, due to the increased concentration of cis-azobenzene molecules. If the sample is kept in the isotropic phase, and then cooled under illumination with violet light, the lowering of the clearing point temperature can be observed by monitoring the transmission of 633 nm light between crossed polarizers. In Fig. 2 we show a typical temperature run. Pump power density was 40 mW/cm^2 at 458nm; the average cooling rate was 1°C/min. The onset of the nematic phase can be clearly observed by the rise of the transmitted light. To standardize the

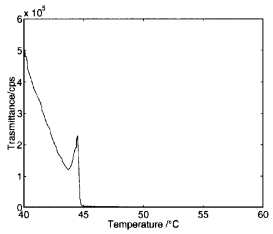

Figure 2: Optical transmittance in crossed polarizers measured at λ=633 nm as a function of the temperature.

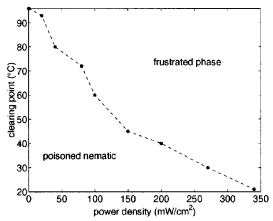

Figure 3: Clearing point as a function of pump power density at λ =488 nm

definition of the clearing point temperature, we define it as the maximum of the derivative of the curve in the neighborhood of the transition.

In Fig. 3 we show the behavior of the clearing point versus the optical pump power density. Such diagram can be seen as a phase boundary between the optically induced isotropic phase and the optically modified nematic phase. Thus for a given temperature and power density the sample can be put in non equilibrium isotropic or nematic phases. For this latter one the order parameters will not be the equilibrium ones, since the optical pump will modify the molecular side chain orientational distribution function [18].

In what follows we shall focus on two typical regions of this phase diagram. The first one is the high temperature region (e.g. $60° < T < 90°$C), where for a given power density (e.g. 40 mW/cm^2) the nematic fluid is in the isotropic phase. This temperature region is reached upon cooling from well within the equilibrium isotropic phase (i.e. from T=130°C). In Fig. 4 we show the time behavior of $R = I_\perp/I_\parallel$. We can identify three main regions in this diagram: in the first, we observe the behavior after the pump light is turned on; the second is the

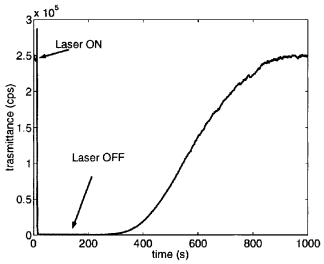

Figure 4: Relaxation of birefringence at 90°C in a pump probe cycle.

incubation period after the pump is turned off, where the signal remains constant; the third is the return to equilibrium. The kinetics of the pump process is first order, as shown by the exponential decrease of the number of equilibrium nematic domains. The characteristic relaxation times for this temperature were studied as a function of pump power and wavelength; the results indicate that there is a definite energy which is necessary to put the nematic fluid in the isotropic phase: for each wavelength the product P·t, where P in the pump power density and t is the transition time, is constant (and equal for example at 90° to an energy density of 44.3 mJ/cm^2 at 458nm). Such energy is furthermore found to be inversely proportional to the sample absorbance.

The incubation period reflects the excess concentration of cis-azobenzenes, over and above the number necessary to frustrate the nematic phase at this temperature. This is shown by the result that the delay time is proportional to the pump energy absorbed. Thus the isotropic phase persists after the pump light is turned off until the thermal back relaxation of the cis molecules reduces their number to the threshold value, after which the nematic phase can exist again. In this incubation period then the characteristic time is given by the thermal cis-trans back isomerization.

Once the threshold value is reached for the nematic phase to exist, the side chain fluid relaxes back to the equilibrium configuration. In this third region, the relaxation dynamics will depend initially still on the cis-trans process, but as time passes more and more on the kinetics of the nematic domain formation and reorientation processes. Such processes, which in a low molecular weight liquid crystal can be very fast (relatively to the time scales we are considering here), are slowed down by the stabilizing effect of the main chain, the second fluid which couples to the azobenzene nematic fluid. Thus the slow characteristic relaxation time we observe in this region should be mainly connected to the conformational rearragements of the main chain which hinder the side chain reorientations which are necessary to form the nematic domains. As we shall see this mechanism is presumably responsible for the extensive high temperature memory effects we have

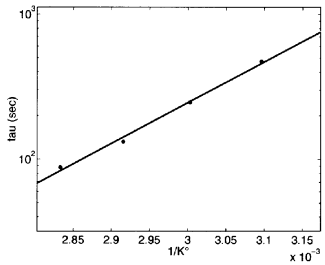

Figure 5: Back-to-equilibrium relaxation times as a function of pump power at some characteristic temperatures.

observed. The return to equilibrium seems to be an ordinary Debye process[19]; data as those of figure 4 were therefore fitted with the relaxation function $f(t) = \frac{1}{1+(\tau/t)^2}$. The corresponding relaxation time τ was obtained, as shown in Fig.5, as a function of pump power for several temperatures in the isotropic part of the phase diagram. The temperature behavior follows an Arrhenius law, with an activation energy E=0.56 eV. Such value is in good agreement with the energy barrier of back isomerization (0.54 eV) reported in the literature [3].

In the second region of the phase diagram (e.g. T< 40°C at 40mW/cm^2), the number of cis molecules created in the photoisomerization process is not sufficient to frustrate the nematic phase. In this situation we have the process of photoinduced reorientation which is amply discussed in the literature, in particular as a function of incident power [16]. Our results are in agreement with those obtained for other polymeric systems. Here we wish to report that measurements at different pump wavelengths do not reproduce the inverse proportionality of the effect to the sample absorbance. The deviation from inverse proportionality in the perturbed nematic phase during the pump part of the cycle is due to the fact that now the cis-trans back isomerization process contributes. In fact the maximum effect takes place at 458nm, which corresponds to the peak in the cis absorption. The photoinduced perturbed nematic phase persists for longer and longer times as the temperature is decreased. In particular, within the limits of our experimental accuracy, we can find no variation in the photo-induced effect on the time scale of several weeks for T$\leq$T$_g$.

The temperature can affect the results of optical pumping in two different ways in the temperature-power range of the phase diagram: first, by affecting the reorientation and relaxation process on several space scales, from molecular side chain reorientations to domain wall dynamics. We shall call this a viscosity effect. Second, due to the temperature variation of the nematic potential we obtain different degrees of molecular order as measured by the nematic parameter S$_2$. We shall call this the nematic potential effect.

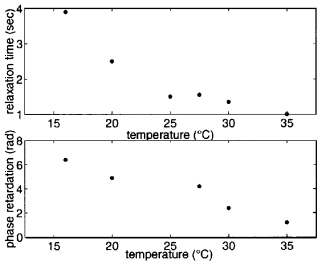

Figure 6: **Top panel:**Relaxation times as a function of sample temperature. **Bottom panel:** Phase shifts achieved at different temperatures (pump power=30 mW/cm^2)

In Fig. 6, top panel, we show the behavior of τ as a function of temperature: this simply reflects the viscosity behavior. The second, aligning, effect is demonstrated in Fig. 6, bottom panel, where we plot the phase difference $\Delta\varphi$.

At low temperatures the phase difference increases since it depends on the order parameter S_2 of the nematic phase. For a sample thickness of approximately 3μm, we have at low temperatures an index of refraction photoinduced anisotropy of 0.1!

The curves in Fig.6 are correlated because both the relaxation times and the phase retardations depend on viscosity. They seem to exibiht a change in the slope aroud T_g, this will be matter of future investigations.

Finally, we wish to discuss the interplay between side chain reorientations and main chain conformational motion. We have performed the following experiment: the virgin sample was brought to the desired temperature in the dark, and the optical anisotropy determined. Thereafter the sample was submitted to the optical pumping which generated the photoinduced , aligned pseudo nematic phase. The sample was then heated to the equilibrium isotropic phase (T=120°C) kept there in the dark for about 30 minutes, then slowly cooled in the dark back to the original starting temperature, whereupon the optical anisotropy was measured. We found that the side chain alignment and the correlated optic axis has resumed the original photoinduced orientation. Furthermore, we found that the memory of the original photoinduced orientation improved with repeated cycles of the sample. This is clear indication of coupling between the side chains fluid and the main chain conformational fluid.

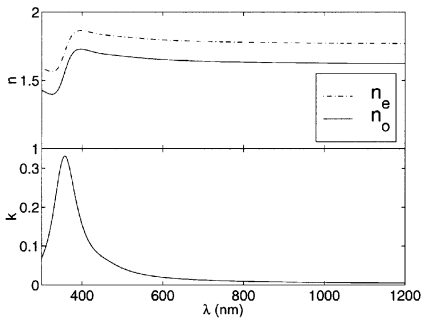

Figure 7: Wavelength dependence of both components of the anisotropic index of refraction (top panel) and absorption constant k for a n=10 LS multilayer of PA4 at room temeprature (bottom panel).

4 Ellipsometry

The measurements were performed both using a single wavelength, high sensitivity null-ellipsometer, and a spectroscopic phase modulated ellipsometer operating in the wavelength range $\lambda = 200 - 1400nm$. As stated, in this paper we shall discuss mainly the spectroscopic data; we refer to our ref.[11] for a presentation of the single wavelength null ellipsometric data. Here we wish to mention that the optical pumping not only changes the index of refraction of the LS deposited multilayers, but also the sample thickness, i.e. volume. The relaxation phenomenology is also found in agreement with that observed with the PIB measurements in the transmission mode.

Here we briefly recall that in an ellipsometric measurement[20] one measures intensity and polarization state of reflected light, as a function of the incident radiation. Given R_p and R_s the reflectivity for p and s light respectively, the ellipsomeric angles Δ and Ψ are defined by $R_p/R_s = tan\Psi e^{i\Delta}$. In the spectroscopic system Δ and Ψ were determined as a function of wavelength by dynamical modulation of the polarization state of the detected reflected light, while the single wavelength measurements were performed by nulling the reflected light, thus achieving perhaps a higher precision at a single wavelength (λ = 633nm, which however is luckily out of the absorption range of the azo-dye).

The measurements were performed on LS multilayers (typically n=10 layers) of PA4 deposited onto clean Si (100) wafers covered by natural SiO_2 oxide. Substrates were carefully characterized prior to film deposition.

We typically found an $\approx$30Å thick oxide layer whose roughness was modelled within the Bruggemann effective medium approximation[21] as a 10Å thick, 50% filled extra-layer. Given this substrate structure, the data from the PA4 multilay-

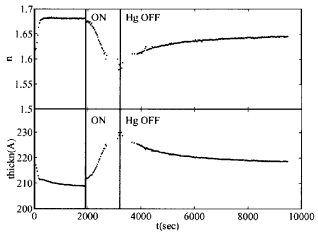

Figure 8: Index of refraction n (top panel) and film thickness (bottom panel, Å) at T=40°C as a function of time, as measured by null-ellipsometry operating at $\lambda = 633nm$. The times at which the Hg lamp was switched ON and OFF are marked by vertical lines.

ers were interpreted assuming a general two damped oscillators model (obeying the Kramers-Kronig relations) which includes both the *trans* and *cis* isomers absorption frequencies and strengths :

$$\epsilon(\omega) = \epsilon_\infty + \Sigma_{j=1}^{2} \frac{f_j \omega_{0j}^2}{\omega_{0j}^2 - \omega^2 - i\gamma_j \omega}$$

where ω is the frequency of the light, ω_{0j} are the energies of the peaks of absorption of the *cis* and *trans* isomers, f_j and γ_j the corresponding oscillator strength and damping factors). From the fit we could extract film thickness, anisotropic index of refraction and wavelength dependent absorption constant, as shown in figure 7. Index of refraction anisotropy was assumed to be uniaxial, directed perpendicularly to the interface. The values obtained are n_e=1.70 and n_o=1.54 for the out-of-plane and the in-plane propagating light respectively (at $\lambda = 633nm$). Other models, isotropic, and anisotropic in plane, were also tested but resulted in worse reproduction of the experimental data. The macroscopic anisotropy of the pristine film probably originates from the Langmuir Schaeffer deposition technique, in which the side chains are oriented perpendicularly to the air/water interface by the applied surface pressure.

We also studied the photo-induced effects on LS multilayers as a function of substrate preparation and sample temperature. In a typical experiment a LS multilayer deposited onto Si substrate was brougth to temperature, left to equilibrate, and then photo perturbed by means of a filtered Hg lamp (λ range around 362 nm). In Fig. 8, we report a typical time evolution of both the index of refraction n (top) and thickness (bottom) for a film made by 10 layers of PA4 deposited on a clean Si substrate. The sample was kept at constant temperature (T=40.0±0.1°C) and was exposed to uv illumination by means of a suitably filtered Hg lamp (λ band=362 ± 5nm). The times at which the uv lamp was switched ON and OFF are marked by vertical lines. The effect of the uv illumination is clearly that of

inducing *trans* to *cis* isomerisation resulting in a marked increase of film thickness (not accompanied by significant roughness increase) and decrease of index of refraction (due to the lower polarizability of the *cis* isomer). Under the experimental conditions reported here, most of the azobenzene side chains have been converted to the *cis* configuration.

5 Discussion and Conclusions

In discussing our results we should like to emphasize three main points: the different relaxation behavior at low temperatures upon approach of the glass transition and above the photoinduced isotropization temperature T_p; the variety of photoinduced effects for T above and below T_p, with particular reference to the morphological and thickness changes, and finally the remarkable memory effects at high temperature.

A preliminary discussion of the first point has already been published[9]; in particular we recall that the relaxation over the microscopic and macroscopic scale was shown to obey the same law as a function of temperature with the same (within experimental error) values for the parameters. Similar results were also obtained from ellipsometric measurements on LS multilayers [11]. In this context particularly relevant are our ellipsometric data, which clearly show that optical pumping induces quite strong changes in the sample thickness, i.e. volume. Thus we can study the approach of the glass transition by varying isothermally the excluded volume fraction and the system cooperativity simply by optical pumping with the appropriate wavelength and intensity.

The second point shows dramatically how well suited PA4 is for applications to optical devices. With relatively small optical intensity (even as small as 1 mW/cm^2) we have several types of huge optical effects: we can reorient optically the optic axis of the system for $T<T_p$; we can also change quantitatively the index of refraction anisotropy. For $T>T_p$, the fast isotropization of the side chain fluid can provide yet another optical writing mechanism. Another important point is the fact that by varying the pump power, we can cross the optically induced phase boundary; this provides an easy write-erase system: we write at low pumping power, we erase at high pumping power, without having to change either temperature or polarization of the pump light.

Finally, a few comments on the high temperature memory effects. A possible explanation of this effect is the coupling of the side chain fluid to the main chains. In particular, the main chain conformation must adapt to the optically induced (hence out of equilibrium) side chain alignment. This adaptation must involve an increased local alignment of the main chain in the direction perpendicular to the side chain orientation plane. Given the much slower main chain conformational dynamics, when the sample is heated into the side chain isotropic phase, the main chains preserve their alignment. When the sample is brought back to the nematic phase, this alignment works as the local anisotropy which tends to align the side chains nematic domains preferentially in the normal plane, thus reproducing the original optical anisotropy.

6 Acknowledgements

We wish to thank prof. M. Warenghem for allowing us to use the facilities of his laboratory for the spectroscopic ellipsometry.

References

[1] A. Blumstein ed., Polymeric Liquid Crystals, Plenum Press, N.Y. (1985) ; N. A. Plat ed., Liquid-Crystal Polymers, Plenum Press, N.Y. (1993)

[2] C. B. Mc Ardle ed.,Side Chain Liquid Crystal Polymers, Blackie and Sons, Glasgow,(1989); V. P. Shibaev, N. A. Plate, Comb-shaped Polymers and Liquid Crystals, Plenum Press, N.Y. (1988)

[3] S. Kumar Chem.Rev. **89**, 1915 (1989)

[4] K. Anderle , R. Birenheide , M. J. A. Werner , J. H. Wendorff 1991 Liquid Crystals **9**, 691 (1991)

[5] J. P. Hansen , D. Levesque , J. Zinn-Justin eds., Liquids, Freezing and Glass Transition, North Holland, Amsterdam (1991);

[6] W. Gotze, J. of Physics: Cond. Matt., **11**, A1 (1999).

[7] C. H. Legge, G. R. Mitchell, J. Phys. D **25**, 492 (1992);

[8] M. P. Fontana, C. Paris, M. Polli , Mol. Cryst. Liq. Cryst. **304**, 207 (1997)

[9] L. Cristofolini, P. Facci, P. Camorani, M. P. Fontana, J. of Physics: Cond. Matt. **11**, A355 (1999)

[10] G. Roberts ed. Langmuir-Blodgett Films (Plenum Press, New York, 1990)

[11] L. Cristofolini, S. Arisi, M.P. Fontana submitted to Phys Rev Lett.

[12] L. Andreozzi, Ph. D. dissertation, University of Pisa (1997)

[13] L. Andreozzi, M. P. Fontana, F. Francia, M. Giordano, D. Leporini, M. Rateo, J. Non-Cryst. Solids, 172-174, 943 (1994)

[14] F.Simoni Nonlinear Optical Properties of Liquid Crystals and Polymer Dispersed Liquid Crystals,World Scientific Singapore, (1997)

[15] Z. Sekkat, J.Wood , E.F. Aust, W. Knoll, W. Volksen, R.D. Miller, Opt. Soc. Am. B **13**, 1713 (1996); J. Stumpe, T. Geue, T. Fischer, H. Menzel, Thin Solid Films **284**, 606 (1996)

[16] S. Hvilsted, F. Andruzzi, C. Kulima, H. W. Siesler, P. S. Ramanujam, Macromolecules, **28**, 2172 (1995)

[17] M. Born, E. Wolf Principles of Optics, Pergamon Press, (1959).

[18] T.G. Pedersen, P.M. Johansen, Phys. Rev. Lett., **79**, 2470 (1997)

[19] P. Debye Polar molecules, Dover Publications, N. Y. (1928)

[20] R. M. A. Azzam, N. M. Bashara, Ellipsometry and Polarized Light North-Holland Personal Library, Amsterdam, (1977)

[21] H. G. Tompkins A user's guide to Ellipsometry Academic press, San Diego, (1993)